Ultrasonic propagation in concentrated colloidal dispersions: improvements in a hydrodynamic model

M. Mahbub Alam

Ultrasonic propagation in concentrated colloidal dispersions: improvements in a hydrodynamic model

M. Mahbub Alam

Laboratory of Waves and Complex Media, UMR CNRS 6294, University of Le Havre, Le Havre, France

Contact: mahbubalam041@gmail.com

Abstract

Recent theoretical and experimental findings demonstrate that modeling ultrasonic attenuation of a concentrated colloidal suspension requires inclusion of shear-induced contributions, an element being unaccounted for by most scattering models. Herein, we extend a hydrodynamic model from low to high particle volume fraction by effectively relating the single particle dynamic drag to particle concentration to account for hydrodynamic inter-particle interactions. We calculate an expression for the complex-valued effective dynamic mass density at high concentrations, which is then combined with a viscosity-corrected effective bulk modulus to estimate ultrasonic velocity and attenuation for a monodisperse suspension of solid spherical particles in a viscous liquid. The effective velocity and attenuation are functions of particle volume fraction, frequency, and physical properties of particles and liquid. We compare our results with those from two recently developed scattering models: a multi-modal multiple scattering model and a core-shell effective medium model, each taking into account the viscosity of the host fluid through shear wave influences. Finally, we find that our extended model predicts experimental attenuation data the best for a silica in water suspension compared to the results of other models.

Keywords: ultrasound, concentrated colloid, acoustic model, viscous liquid, hydrodynamics

Graphical abstract

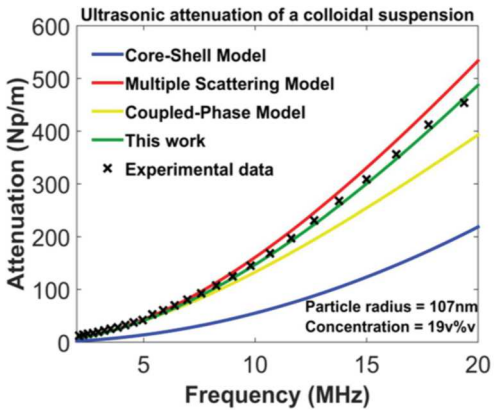

1. Introduction

Ultrasound spectroscopy is an effective experimental tool used to extract information (e.g. particle size and concentration) about colloidal suspensions. It has opened the door to multiple industrial applications, such as ceramics, food, chemicals, minerals, and pharmaceuticals, among others. [1]

This technique enjoys several advantages over other analytical tools such as the widely used light diffraction technique in that it can be employed in systems that are concentrated, optically opaque, and electrically non-conducting. Experimental spectroscopic measurements require interpretation and characterization which mostly come from theoretical models. Mathematical models relate experimentally observable quantities (e.g. attenuation and velocity) of a colloid to the experimentally inaccessible quantities (e.g. volume fraction and compressibility). The problem of predicting ultrasonic properties of particulate dispersions is long-standing and highly important, especially at high particle volume fractions. [2, 3] Most theoretical treatments are limited to dilute systems, and either focus on inviscid fluid host cases or consider viscosity without taking inter-particle interactions into consideration, thereby severely limiting their usefulness. Here, we investigate underlying mechanisms in dense colloids by extending a hydrodynamic model.

Epstein and Carhart [4] and Allegra and Hawley [5] developed a scattering theory (known as ECAH theory) that is widely used to model attenuation; however, this theory treats each particle as isolated, disregards interactions among particles, and breaks down at high particle concentrations, low frequencies or large particle sizes. [2, 6] Multiple scattering theory, [7–12] on the other hand, takes account of multiple scattering effects, meaning that scattered waves from one particle can reach its neighboring particles and can undergo rescatterings. This theory is grounded on the quasi-crystalline approximation (QCA) [13] and can satisfactorily predict ultrasonic properties of a particulate system from low to moderate concentrations. Since this theory is built around the idea that particle concentration be small and effective properties be expressed in terms of integer powers of particle concentration, despite the incorporation of pair-distribution functions, [8, 14] it fails at very high concentrations. [2] Using the principles of hydrodynamic theory, Ament obtained a complex-valued frequency-dependent expression for effective density, which appreciably differs from the traditional assumption of volume-averaged mass density. [15] In an attempt to model acoustic propagation through a concentrated dispersion of solid particles in a liquid, Harker and Temple formulated a coupled-phase model through consideration of bulk hydrodynamic properties of a suspension and calculated an effective compressional wavenumber. Their model takes account of fluid viscosity and is valid when the particle size is smaller with respect to the acoustic wavelength. This model, however, was found to give a lower level of agreement with experimental data than that of the ECAH model. [2, 16] A recent study by Valier-Brasier *et al.* [17], through an extension of a coupled-phase model and the ECAH model for a suspension of solid and liquid particles, showed analytically and numerically that ultrasonic propagation parameters predicted by both types of model give identical results in the dilute limit.

One of the factors that confine conventional multiple scattering models to apply to dense particulate dispersions is the negligence of multiple scattering of additional wave modes (e.g. shear wave) produced at the surface of each particle from the incident compressional wave mode.

Recently, Luppé *et al*. formulated a multi-modal multiple scattering theory by incorporating the effect of wave mode conversion into their model [18, 19]; they considered rescatterings of shear waves produced at one particle by a nearby particle. Experimental findings by Forrestal *et al.* [20] for a suspension of silica spheres in water corroborated attenuation values predicted by this model. In an attempt to understand the effect of wave mode conversion on the effective properties of a suspension, Alam *et al*., [21] based on the coherent potential approximation (CPA), developed a core-shell effective medium model incorporating shear wave contributions into the model and calculated the effective bulk modulus and density. This work, however, has yet to investigate ultrasonic speed and attenuation.

In this article, we investigate ultrasound velocity and attenuation for a concentrated suspension of solid spheres in a viscous liquid by taking inter-particle interaction into account. Our motivation comes from the need to benchmark the recently developed multimodal multiple scattering model of Luppé *et al.* [18] using a different approach and to develop a model applicable to highly concentrated suspensions due to multiple scattering models being inherently restricted to the low-concentration assumption. To this end, instead of developing a new model, we focus on identifying and removing the limitations of the existing hydrodynamic theory. We extend a hydrodynamic model (as discussed above) developed by Ament and adapt it to high particle concentration. Ament model calculates effective dynamic density by incorporating viscosity of the host fluid through an isolated-particle drag form, thereby neglecting hydrodynamic interactions among inclusions which restricts the model to low particle concentration. In order for the model to be applied to a concentrated suspension, here we update the drag by including the presence of other neighboring particles, thus relating it to the particle concentration; we then use a viscosity-modified bulk modulus from a scattering model to estimate the effective attenuation and speed. Since effective medium models are not restricted to low concentration, here we also examine the core-shell model recently formulated by Alam *et al*. and calculate an effective wavenumber from this model to investigate ultrasonic attenuation and velocity. The coupled-phase model of Harker and Temple built for concentrated suspensions is also studied. Recent experimental attenuation data for silica spheres in water is compared with the predictions of all four models.

2. The models

2.1. Modified hydrodynamic

Hydrodynamic models have some advantages over scattering models in predicting dynamic properties of a concentrated, viscous suspension. Unlike multiple scattering models that are valid only up to a limited concentration due to the low concentration assumption, hydrodynamic models, being self-consistent, do not have any constraint on particle concentration and can thus be used to determine the dynamic properties of a colloid at very high concentrations. Since most existing hydrodynamic formulations for solid suspensions are either limited to dilute cases [15, 17, 22] or suffer from poor modeling, [2, 23] here we extend a hydrodynamic model due to Ament from dilute to dense systems and estimate the ultrasonic attenuation and velocity of a two-phase concentrated suspension. Ament, using a simple yet elegant approach, derived an expression for the effective dynamic density inclusive of viscous effects. [15] He modeled the suspension in terms of volume-averaged values of local velocity and momentum. Combining equations of incompressible flow, conservation of momentum, and equilibrium between the dynamic drag on a sphere (which includes both inertial and viscous terms) and the rate of momentum transfer between the particle and the surrounding liquid, Ament arrived at a formula for the effective density, which, for a monodisperse suspension of spheres, is given by

$$\rho_{eff} = (1-\varphi)\rho + \varphi\rho' - \frac{(\rho'-\rho)^2\varphi(1-\varphi)}{\rho'(1-\varphi)+\rho\varphi+\rho S}, \tag{1}$$

$$\text{where } S := \frac{1}{2} + \frac{9}{4}\left[\frac{1}{\beta a} + i\frac{1}{\beta a}\right] + i\frac{9}{4}\left(\frac{1}{\beta a}\right)^2. \tag{2}$$

Here, $\beta = \sqrt{\rho\omega/2\eta}$, a is the particle radius, η the shear viscosity of the base fluid, φ the particle volume fraction, and ω the angular frequency; ρ' and ρ are the densities of the particle and the liquid, respectively. The reciprocal of β is an important parameter known as the viscous boundary layer; its thickness compared to the inter-particle distance is a measure of the importance of viscous effects. It is of note that Ament's paper suffers from some typographical errors and hence care should be taken when equations of this paper are used.

Here, the factor, S, furnishes us with information regarding the nature of the hydrodynamic interaction among oscillating particles. It has three components: the first is the added mass term arising from the relative acceleration between the particle and the fluid; the second is related to the Basset/history force stemming from the unsteady diffusion of vorticity within the boundary layer around the particle; and the last is the Stokes' drag due to the viscous force acting on the particle. [24] S, being independent of particle concentration, is valid for dilute suspensions only, where each particle is effectively isolated. When a particle moves relative to a liquid material, it gives rise to a hydrodynamic field and produces a sliding motion of the liquid in its immediate vicinity. The region

in which this disturbance takes place is called the hydrodynamic boundary layer. As the concentration of the suspension increases, the average separation distance between particles reduces. When the thickness of the boundary layer becomes comparable to the inter-particle separation, the particles begin to interact with each other through their respective hydrodynamic fields. Therefore, to model concentrated suspensions, the hydrodynamic interaction term S needs to be modified and effectively related to the particle volume fraction.

Since Eq. (2) is derived on the assumption of unsteady creeping flows, the Stokes' drag must be modified when a particle is in a suspension. Richardson and Zaki [25] determined the Stokes correction factor to be $(1-\varphi)^{-4.65}$, as we will demonstrate, this will serve our purpose to model attenuation effectively. Although the history/Basset force for a single sphere has been investigated by a number of authors, [24, 26–28] an expression to account for the concentration dependency of the force is not known and most probably does not exist in the literature. Since the effect of Basset force with respect to that of the Stokes' force or inertial force is smaller, one can safely use the isolated-sphere form of the history force. Regarding the coefficient of the added (virtual) mass force, Harker and Temple used the Zuber's correction factor (as discussed below), [29] which is derived using a cell model and is valid for a suspension of bubbles/droplets in liquids. [30, 31] This expression for the solid-in-liquid system significantly overestimates the effect of the added mass force at high concentrations. Zuber's result is

$$S_{add,z} = \frac{1}{2}[1 + \mathcal{L}_Z(\varphi)\,], \tag{3}$$

$$\text{with } \mathcal{L}_Z(\varphi) := \frac{3\varphi}{1-\varphi}. \tag{4}$$

Recently, Gus'kov, [32] taking account of pairwise interactions between spheres, calculated the added mass force experienced by a particle of arbitrary mass in a suspension. Using his correction in the leading order of particle volume fraction, the added mass term can be written as

$$S_{add,G} = \frac{1}{2}[1 + \mathcal{L}_G(\hat{\rho},\, \varphi)\,], \tag{5}$$

$$\text{with } \mathcal{L}_G(\hat{\rho},\, \varphi) := \left[\frac{7}{48} - \frac{4245}{11264}\frac{1-\hat{\rho}}{1+2\hat{\rho}} + \frac{40}{11264}\frac{(1-\hat{\rho})^2}{(1+2\hat{\rho})^2}\right]\varphi, \tag{6}$$

where $\hat{\rho} = \rho'/\rho$ is the density ratio. For a silica-in-water colloid, $\hat{\rho} \simeq 2.1$, and for 20% particle volume fraction, $\varphi = 0.2$, which gives $\mathcal{L}_G \simeq 0.045$ and $\mathcal{L}_Z \simeq 0.750$; therefore, according to Gus'kov and Zuber, the added-mass force of a silica sphere in a suspension increases by an amount of 4.5% and 75%, respectively. Zuber's result for a solid-in-liquid system clearly produces unphysical results at high concentrations. Our analysis, using Gus'kov's result, shows that this contribution of the added mass even for $\varphi = 0.6$ to the overall change in the effective attenuation (which is sensitive) is of no real consequence. Also, the added-mass force is a second-order effect when compared with the Stokes drag, hence we can use the isolated-sphere form of the added mass coefficient as well, which is simply 1/2. A plausible explanation is that the inertial force being conservative is not

associated with loss and hence does not contribute to attenuation (which is predominantly viscous). After the systematic analysis, we thus write the modified interaction term as

$$S = \frac{1}{2} + \frac{9}{4}\left[\frac{1}{\beta a} + i\frac{1}{\beta a}\right] + i\frac{9}{4}\left(\frac{1}{\beta a}\right)^2 (1-\varphi)^{-4.65}. \quad (7)$$

Recent studies have found that continuum theory remains valid to study nanoscale flows in a channel with size as small as 50 nm. [33, 34] Since we here are not investigating confined flows, the mechanical models, such as Richardson and Zaki and Gus'kov, can be safely applied to spheres as small as 50 nm in radius.

Since the Ament model calculates effective density, an expression for the effective bulk modulus is needed to obtain an expression for the effective compressional wavenumber. Hydrodynamic models, being unable to calculate the effective bulk modulus of a suspension, assume a volume-averaged compressibility or a harmonic (or Reuss) average of bulk modulus, [2, 23]. By contrast, scattering theory shows that the effective bulk modulus for a viscous suspension slightly differs from its inviscid counterpart [21, 35] and thereby affects ultrasonic attenuation and velocity to a noticeable extent. To calculate the effective wavenumber, we, therefore, choose to use the viscosity-corrected, effective bulk modulus expression of Ref. [21] which is given by

$$\frac{B_{eff}}{B} = \frac{(k_c a)^2\left[\varphi\,(k_s a)^2\,k_c a + 4iT_0^{cc}\right]}{(k_s a)^2\left[\varphi\,(k_c a)^3 - 3iT_0^{cc}\right]}. \quad (8)$$

Here, B is the bulk modulus of the liquid, T_0^{cc} is the monopole scattering coefficient of the compressional wave, $k_c = \omega/v + i\,\alpha$ and $k_s = \sqrt{\rho\omega/2\eta}\,(1+i)$ are the compressional and shear wavenumbers in the liquid, v is the compressional wave speed, and α is the attenuation coefficient. It can be noted that Eq. (8), when expressed in terms of the Lamé parameters through k_c, k_s, and T_0^{cc}, takes the well-known effective bulk modulus form obtained by Kuster and Toksöz for a solid-in-solid system. [21, 36] We prefer the form of Eq. (8), because it captures more information about attenuation, such as the bulk viscosity, through the monopole scattering coefficient and the wavenumbers, and can effectively model attenuation even for small particles, as we shall see.

Since the wavelength of shear (viscous) waves in the liquid is much smaller than that of shear waves in the solid, or of compressional waves in the liquid, an effective compressional wavenumber ξ can be approximated as

$$\xi^2 = k_c^2\,\frac{\rho_{eff}}{\rho}\,\frac{B}{B_{eff}}. \quad (9)$$

Therefore, Eq. (9) with Eqs. (1), (7) and (8), can be written as

$$\xi^2 = \frac{k_c^2}{\rho}\,\frac{(k_s a)^2\left[\varphi\,(k_c a)^3 - 3iT_0^{cc}\right]}{(k_c a)^2\left[\varphi\,(k_s a)^2\,k_c a + 4iT_0^{cc}\right]}\left\{(1-\varphi)\rho + \varphi\rho' - \frac{(\rho'-\rho)^2\varphi(1-\varphi)}{\rho'(1-\varphi)+\rho\varphi+\rho\left[\frac{1}{2}+\frac{9}{4}\left(\frac{1}{\beta a}+i\frac{1}{\beta a}\right)+i\frac{9}{4}\left(\frac{1}{\beta a}\right)^2(1-\varphi)^{-4.65}\right]}\right\}. \quad (10)$$

The effective velocity and attenuation are given by $\mathrm{Re}(\omega/\xi)$ and $\mathrm{Im}(\xi)$ respectively. Since Brownian diffusion has a second-order effect on hydrodynamic interaction for a very dilute

suspension of small particles, [37] here its effect on ultrasonic velocity and attenuation is assumed to be negligible. It is noted that the model is not valid for concentrations of particles that are too dilute such that the interparticle distance becomes larger than the wavelength of the compressional wave.

To summarize, we have extended Ament's model from dilute to dense systems by incorporating hydrodynamic particle-particle interaction into the model and calculated effective dynamic density. An effective bulk modulus inclusive of both bulk and shear viscosity obtained from a scattering model is then combined with the effective density to estimate ultrasonic velocity and attenuation for a dense suspension of solid spheres in a viscous fluid.

2.2. Harker and Temple

To estimate ultrasonic propagation parameters for monodisperse suspensions of solid particles, Harker and Temple developed a coupled-phase model based on hydrodynamic principles.[23] The model was investigated by a number of authors[2, 16] for ultrasonic velocity and attenuation and found to differ significantly from the experimental data. As the model neglected heat conduction, the discrepancy was primarily attributed to the negligence of thermal effects for both emulsions and suspensions. Since for a high-density contrast ($\hat{\rho} > 2$) dispersion, thermal effects are of less significance compared to viscous effects, [5, 38] we here compare the model with the modified Ament model and indicate that the disagreement of the Harker and Temple model with the experimental data is mainly due to the poor modeling of the hydrodynamic interaction among particles rather than the disregard of thermal effects.

The coupled-phase model assumes that the ensemble of the particles forms a single continuum and the base liquid does the other so that each phase can be described by average properties, without any spatial coordinate. Upon employment of the conservation of linear-momentum and mass equations for both phases separately, and incorporating the drag force on one phase caused by the other into the momentum equations, Harker and Temple obtained four governing differential equations for the two-phase suspension. In the presence of an ultrasonic field, state variables - such as velocity, density, and pressure - are assumed to have small perturbations from their (static) equilibrium values. Expressing each state variable as the sum of its equilibrium value plus a small perturbation, and solving the resulting set of equations, they obtained the following expression for the effective compressional wavenumber for the particulate mixture:

$$\xi^2 = \omega^2[(1-\varphi)\kappa + \varphi\kappa']\frac{\rho[\rho'(1-\varphi+\varphi S)+\rho S(1-\varphi)]}{\rho'(1-\varphi)^2+\rho[S+\varphi(1-\varphi)]}, \tag{11}$$

$$\text{where } S := \frac{1}{2}\left(\frac{1+2\varphi}{1-\varphi}\right) + \frac{9}{4}\left[\frac{1}{\beta a} + i\frac{1}{\beta a}\right] + i\frac{9}{4}\left(\frac{1}{\beta a}\right)^2, \tag{12}$$

Here κ and κ' are the compressibilities of the liquid and the particle, obtained from $\xi^2 = \rho\kappa\omega^2$ and $\xi^2 = \rho'\kappa'\omega^2$ in the limit of $\varphi = 0$ and $\varphi = 1$, respectively. Eq. (11) is the dispersion relation that relates the effective compressional wavenumber to the physical properties of the component phases

of the suspension as well as to the interaction between them. As the model uses volume-averaged conservation equations for each phase, the effective wavenumber matches the wavenumber of the dispersed phase if the particle volume fraction is set to 100%, and the model is thus self-consistent. The assumption that all the particles in the mixture constitute a continuum restricts the model to the long-wavelength regime (i.e. $k_c a \ll 1$). The model takes into account the hydrodynamic interaction among particles through S and is thus valid for concentrated suspensions. The viscous interaction is included in the Stokes drag and the Basset history force through Vand's effective viscosity formula,[23] so the particles can suspend in a fluid of viscosity equal to that of the suspension as a whole, instead of the viscosity of the base fluid. Vand's effective viscosity expression for spherical particles is

$$\eta_{eff} = \eta(1 + 2.5\varphi + 7.349\varphi^2 + \cdots). \tag{13}$$

Harker and Temple used $\beta = \sqrt{\rho\omega/2\eta_{eff}}$ to evaluate S instead of the viscosity of the continuous phase η. Since the added-mass term in S does not contain the fluid viscosity, Harker and Temple used Zuber's added mass coefficient to account for the particle-particle interaction due to the inertial effect. As explained above, Zuber's expression overpredicts the effect of added-mass interaction among solid particles in a liquid.

2.3. Multi-modal multiple scattering

The multi-modal multiple scattering model formulated by Luppé *et al.* incorporates the effects of the reconversion of a shear wave mode into the model, which is in contrast with the traditional scattering models, such as ECAH, [4, 5] Lloyd and Berry,[9] and Waterman and Truell, [7] where the scattering of a compressional wave is considered only, disregarding shear wave contributions. Although the shear wave decay length at low concentrations (and/or high frequencies) is small compared to the average interparticle distance, at high concentrations (and/or low frequencies) the shear wave produced at one particle, due to a longer decay length, can get rescattered by an adjacent particle, converting back into the compressional wave mode which contributes to the overall effective compressional wave field and consequently affects ultrasonic attenuation and velocity.

While Forrester *et al.* have recently compared ultrasonic attenuation predictions from the multimodal multiple scattering model with the experimental data and with the predictions of the single-mode multiple scattering model of Lloyd and Berry, the effective velocity remains to investigate. Also, the model needs to be compared with other concentrated, visco-acoustic models because the Lloyd and Berry model does not account for the effect of wave mode conversion and is thus limited to inviscid base fluid suspensions and low concentrations. Here we investigate both attenuation and velocity predictions of the multimodal multiple scattering model by comparing them with those of the other concentrated models inclusive of shear waves. According to the formulation,

the effective compressional wavenumber, inclusive of shear-induced effects, up to third order in concentration can be written as

$$\xi^2 = k_c^2\left[1 - \frac{3i\varphi}{(k_c a)^3}(T_0^{cc} + 3T_1^{cc}) - \frac{27\varphi^2}{(k_c a)^6}(T_0^{cc}T_1^{cc} + 2T_1^{cc}T_1^{cc}) + \Delta_2^{cs} + \Delta_3^{cs}\right], \tag{14}$$

with $$\Delta_2^{cs} := -\frac{27i\varphi^2}{(k_c a)^6}\frac{k_c^3 b}{(k_c^2 - k_s^2)}\Omega\, T_1^{cs}T_1^{sc}, \tag{15}$$

$$\Delta_3^{cs} := -\frac{81i\varphi^3}{(k_c a)^9}\frac{k_c^6 d^2}{(k_c^2 - k_s^2)}\Omega^2\, T_1^{cs}T_1^{sc}T_1^{ss}, \tag{16}$$

$$\Omega := k_c d\, j_0'(k_c d)\, h_0(k_s d) - k_s d\, j_0(k_c d)\, h_0'(k_s d), \tag{17}$$

where $d = 2a$ is assumed to avoid the overlapping among spheres, with a being the particle radius; $i = \sqrt{-1}$ is the imaginary unit, j_0 and h_0 are zero order Bessel and Hankel functions; T_n^{pq} (presented in the Appendix) is the nth order partial wave scattering coefficient of a scattered wave of mode $q = c$ or s produced from an incident wave of mode $p = c$ or s. [39] Δ_2^{cs} and Δ_3^{cs} are additional terms in the model that include the mode-conversion (acoustic-shear) contributions; in the high frequency or long shear wavelength limit, these two terms vanish, and Eq. (14) reduces to the effective wavenumber for solid particles in inviscid liquid suspensions, as given by the Lloyd-Berry model. [9] Although the multiple scattering model is valid for arbitrary frequencies, Eq. (14) is simplified under the condition that the compressional wavelength is much smaller than the particle radius a, (however, no assumption is made regarding the shear wavelength). Therefore, the total scattering is approximated by retaining the monopole and dipole modes only. The multiple scattering model is not self-consistent in that the particle volume fraction does not approach 100%. The model assumes a low concentration assumption to derive the effective wavenumber. Full details of the model can be found in Ref. [18].

2.4. Core-shell

Alam *et al.,* based on the partial wave analysis, have recently developed a core-shell, self-consistent effective medium model for a suspension of solid spheres in a viscous fluid.[21] They have incorporated the viscosity of the base fluid through shear waves into the model and have found the viscosity to produce an appreciable effect on the effective bulk modulus and density. Since this model has not yet investigated the effective velocity and attenuation, here we examine these acoustic properties by comparing them with other visco-acoustic models and experimental data to see the suitability of the model in predicting dynamic properties.

The colloidal suspension is modeled as a particle surrounded by a shell of viscous base liquid which itself is embedded in a homogeneous medium having the same effective properties as the suspension as a whole, thereby reducing the many-particle problem to a single-particle one. The shell radius b is related to the particle radius a through the concentration of the whole suspension by $\varphi = (a/b)^3$; the more particles are in the suspension, the thinner the shell becomes and vice versa.

Thermal effects have been neglected on account of high-density-contrast suspensions. To derive effective properties, the wavelength of the acoustic wave is considered to be much smaller than the shell radius and the interparticle spacing between particles. Assuming that the scattering characteristics of the core particle are known, continuity of the radial and tangential displacements and stresses at the boundary between the shell and the effective medium is imposed for each Rayleigh partial wave order independently. Since viscous liquids support shear waves, mode conversion is accounted for by including shear waves along with the compressional waves in the boundary equations. The self-consistent solution is then sought by invoking the coherent potential approximation such that the core-shell system within the effective medium generates no scattered waves in the lowest orders of scattering coefficients. The monopole and dipole modes are the dominant scattering modes in the long-wavelength limit. For an incident compressional wave, an effective bulk modulus B_{eff} is derived from the monopole mode and an effective density ρ_{eff} from the dipole mode, which are respectively given by:

$$B_{eff} = \frac{B(k_c b)^3 + 4i\mu T_0^{cc}}{(k_c b)^3 - 3iT_0^{cc}} \tag{18}$$

$$\rho_{eff} = \frac{N}{D}, \tag{19}$$

with $N := 6(T_1^{cc}T_1^{ss} - T_1^{cs}T_1^{sc})[k_s b h_1'(k_s b) + 2h_1(k_s b)]$

$$+6T_1^{cc}[k_s b\, j_1'(k_s b) + 2j_1(k_s b)] - 3k_c b\, T_1^{sc} - 6\frac{T_1^{cs}(k_c b)^2}{(k_s b)}$$

$$+\mathrm{i}(k_c b)^3 T_1^{ss}[h_1(k_s b) - k_s b h_1'(k_s b)] + \mathrm{i}(k_c b)^3[j_1(k_s b) - k_s b j_1'(k_s b)], \tag{20}$$

and

$$D := 3(T_1^{cs}T_1^{sc} - T_1^{cc}T_1^{ss})[k_s b h_1'(k_s b) - 7h_1(k_s b)]$$

$$-3T_1^{cc}[k_s b\, j_1'(k_s b) - 7j_1(k_s b)] - 3k_c b\, T_1^{sc} - 6\frac{T_1^{cs}(k_c b)^2}{(k_s b)}$$

$$+\,\mathrm{i}(k_c b)^3 T_1^{ss}[h_1(k_s b) - k_s b h_1'(k_s b)] + \mathrm{i}\,(k_c b)^3[j_1(k_s b) - k_s b j_1'(k_s b)]. \tag{21}$$

where $\mu = -i\omega\eta$ is the shear modulus of the liquid. Since shear waves do not exist in the monopole mode, the viscosity of the base fluid is included in the complex Lamé parameters. An effective compressional wavenumber for the core-shell model can be calculated from Eq.(9) using Eq.(18) and Eq.(19) with Eq. (20) and Eq. (21). Although the application of the self-consistent condition restricts the model to the long-compressional wavelength region, no such restriction is placed on the shear wavelength. Unlike the case of a solid medium, the shear wavelength in a viscous liquid is not the same order of magnitude as the compressional one, which allows one to investigate a broad range of shear wavelengths while at the same time staying in the long compressional wavelength regime, thus observing the dynamic behavior of the effective velocity and attenuation. The model is not restricted to a certain concentration range, but the long compressional wavelength assumption places a limit on frequency and particle size, which depends on the concentration. Details of the model can be found in the original paper. [21]

3. Results and discussions

Numerical calculations are performed in Matlab for silica spheres in water at 25°C. The physical properties of silica and water are used from Ref. [20]. Ultrasonic attenuations as a function of frequency calculated from the above four models are compared with the experimental attenuation data of silica spheres in water obtained from Ref. [40]. Here we use particle densities of 2280 kg.m^{-3}, 1980 kg.m^{-3}, 1986 kg.m^{-3}, and 2041 kg.m^{-3} for particle radius of 50 nm, 107 nm, 215 nm, and 500 nm, respectively to plot Figure 1 to compare with the experimental data. We also plot attenuation as a function of particle concentration and ultrasonic velocity as functions of frequency and particle volume fraction. For these plots, we use a fixed particle density of 2041 kg.m^{-3} because we compare theoretical predictions from each model. The computational data for the four models is available in Ref. [41]. As each of the four models is studied for the long-compressional wavelength approximation, for the simplicity of the numerical calculation, we have used the closed-form analytical expressions for the multimodal scattering coefficients [21, 39] (given in the Appendix) rather than obtaining them numerically from the matrix-inversion of boundary equations to evaluate the effective wavenumbers from the multiple scattering model and the core-shell model.

A Malvern Ultrasizer MSV spectrometer operated in a through-transmission ultrasound mode in the experiment. The system used two pairs of transmitting and receiving transducers. Four samples of silica particles with radii 50 nm, 107 nm, 215 nm, and 500 nm were used; using a helium pycnometer, their respective densities were found to be 2280 kg.m^{-3}, 1980 kg m^{-3}, 1986 kg.m^{-3}, and 2041 kg.m^{-3}. Deionized water was used to carry out calibration. Sample volumes of 500 mL were prepared. The homogeneity of the samples was retained throughout the experiment using an agitator and the temperature of the samples was kept at 25 ± 0.2 ℃. The ultrasonic attenuation coefficient was calculated as a function of frequency over the range of 1-20 MHz. The experimental details are given in the original paper. [20]

3.1. Dependence of attenuation on frequency

We first explore the effective attenuation as a function of frequency up to 20 MHz for four different particle concentrations. It can be seen from Figure 1 that attenuation results from the modified Ament model and the multimodal multiple scattering model show excellent agreement with the experimental data. For small particle sizes, the modified Ament model even gives a better fit than the multiple scattering model. Except for the suspension of 50 nm particle radius, attenuations predicted by the Harker and Temple model fall considerably below the experimental values. The core-shell model deviates dramatically from the experimental attenuation results and the other three predictions across the whole frequency range in all four cases.

The multiple scattering model owes its success to the inclusion of shear wave contributions. The shear wave mode, generated from the acoustic mode at one particle, can reach its neighboring particles and undergo rescattering, which, from a hydrodynamic point of view, amounts to the overlapping of viscous boundary layers. In order to effectively model attenuation, we thus justify our concentration-dependent correction to the Stokes drag in modifying Ament's model and the use of a viscosity-corrected bulk modulus to calculate the effective compressional wavenumber.

The disagreement between the results of Harker and Temple's theory and experimental results may be an overestimation of the added-mass force's contributions at high concentrations; also, their use of Vand's effective viscosity expression instead of the liquid's viscosity to account for viscous interaction is questionable. Austin *et al.* found the attenuation results of the Harker and Temple model to greatly differ from their experimental findings for silica-in-water, iron-in-water, and kaolin-in-water systems. [16] They attributed this deviation to the negligence of thermal waves, which, however, probably has more to do with proper viscosity incorporation than the exclusion of thermal waves for solid-in-liquid systems. The marked deviation of attenuation predicted by the core-shell model is suspected to be the overestimation (resp. underestimation) of shear-compressional conversion, reducing (resp. increasing) the overall attenuation.

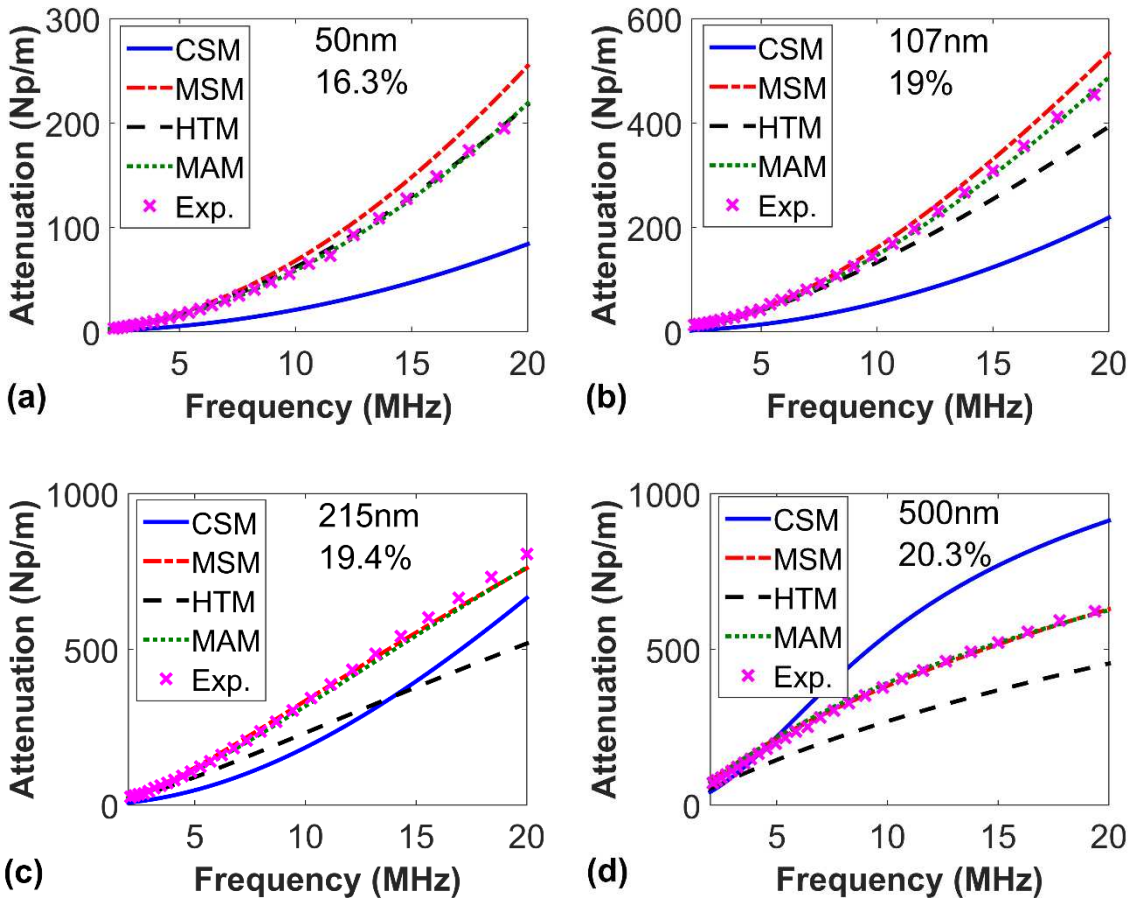

Figure 1. Comparison of experimental attenuation data with those predicted by the core-shell model (CSM), the multiple scattering model (MSM), Harker and Temple model (HTM), and modified Ament model (MAM) for silica spheres in water as a function of frequency for a suspension of (a) particle radius 50 nm at 16.3v%v, (b) of particle radius 107 nm at 19v%v, (c) of particle radius 215 nm at 19.4v%v (d) of particle radius 500 nm at 20.3v%v.

3.2. Dependence of attenuation on concentration

In order to investigate attenuation in more detail, we now explore the concentration dependency on effective attenuation. Figure 2 illustrates how the attenuation varies with concentration at a fixed frequency up to concentration 40v/v% for two different particle sizes. For the 100 nm particle radius suspension, the attenuations from the modified Ament model and the multiple scattering model agree well with each other, while the Harker and Temple model shows agreement up to about a concentration of 25v/v% with these two models and then starts to disagree. On the other hand, the core-shell model markedly underestimates the attenuation despite showing agreement with the other three models at low concentrations. Regarding the suspension of 1 μm particle radius, again, attenuations predicted both by the modified Ament model and by the multiple scattering model match reasonably with each other, while results from the other two models are significantly different than these two models. The core-shell model predicts attenuation values which are complicated, exhibiting a fractional power concentration dependence which is a fingerprint of such models. The Harker and Temple model (as discussed above) suffers on account of not effectively including the hydrodynamic interactions into account.

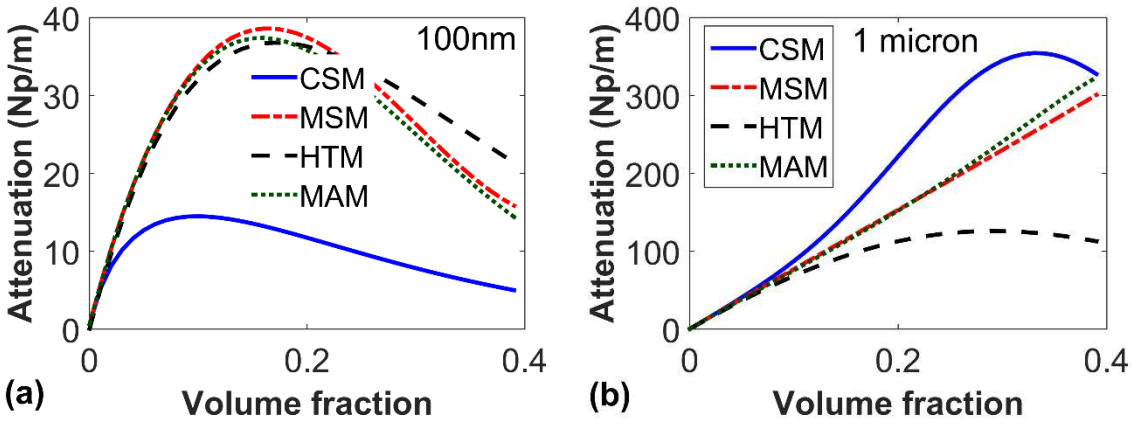

Figure 2. Attenuation as a function of particle volume fraction at 5 MHz frequency for a suspension of particle radius (a) 100 nm and (b) 1 μm.

3.3. Dependence of velocity on frequency

In order to observe the dispersive nature of ultrasonic waves, we graph ultrasonic velocity over a frequency range of $f \in [10^{-2}, 40]$ MHz for a suspension of particle radius $a = 1\ \mu m$ predicted by each model for two different values of concentration: $\varphi = 0.1$ and $\varphi = 0.2$. It can be seen from Figure 3 that phase velocities predicted by each model qualitatively exhibit a very similar behavior. The velocity shows a plateau in the low-frequency region, followed by a smooth and considerable increase in the intermediate-frequency range, and then almost levels off in the high-frequency region. Such a behavior is characteristic of ultrasonic velocity in a suspension. Since the effective bulk modulus has a small frequency dependency (quasi-static), the dynamic behavior of the ultrasonic speed is in large part caused by the dynamic nature of the effective density. The upper and lower limits of the speed are determined by the low-frequency (viscous/Stokes) and high-frequency (inertial/inviscid) regimes of the real part of the complex-valued dynamic density.

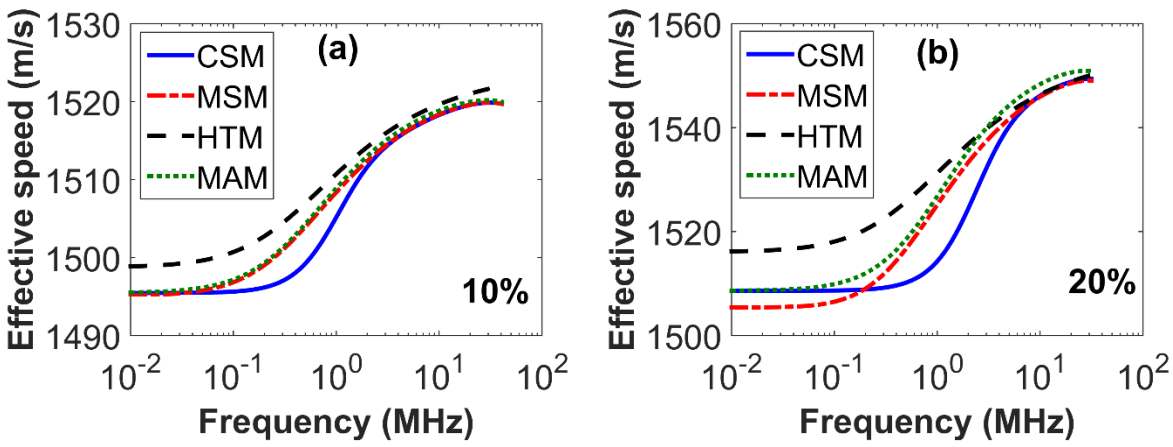

Figure 3. Ultrasonic velocity as a function of frequency for a monodisperse suspension of particle radius 1 μm for a particle volume fraction of: (a) 10% and (b) 20%.

At low concentrations, ultrasonic velocities predicted by both the multiple scattering model and the modified Ament model agree with each other across the entire frequency range. The core-shell model, except the intermediate-frequency region, also shows excellent agreement with these two models. Velocity from the Harker and Temple model in the low-frequency region shows a noticeable disagreement from the other three predictions, which can possibly be attributed to the assumption of volume-averaged compressibility which is true for an inviscid base fluid but not for a viscous one. At higher concentrations, again, both the modified Ament model and the multiple scattering model show the same level of agreement except a slight discrepancy in the low-frequency range, while the Harker and Temple model shows a noticeable deviation from the other three models at both concentrations.

3.4. Dependence of velocity on concentration

To see what effect concentration has on effective velocity, we have graphed (in Figure 4) the ultrasonic speed against particle volume fraction at a fixed frequency of 5 MHz for a suspension of particle radius: $a = 100\ nm$ and $a = 1\ \mu m$. For the $100\ nm$ particle colloid, the core-shell model and the modified Ament model almost coincide on the same curve across the whole concentration range because they both use the same effective bulk modulus; while the multiple scattering model, after agreeing with these two models, starts to be at odds from about 20v%v. Results from the Harker and Temple model show an appreciable disagreement from the other predictions.

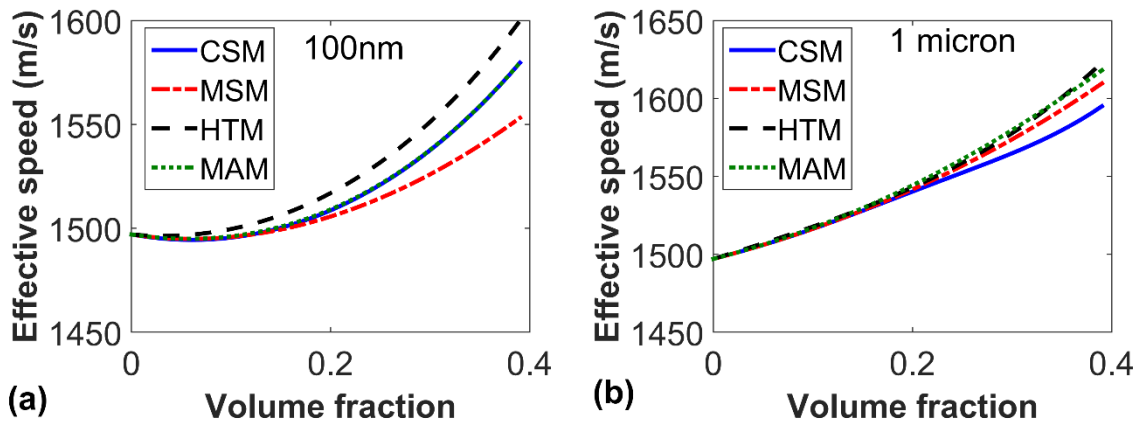

Figure 4. Ultrasonic velocity as a function of particle volume fraction at 5 MHz frequency for a suspension of particle radius (a) 100 nm and (b) 1 μm.

As to the $1\ \mu m$ particle suspension, results from each model show agreement up to about 25% volume fraction. It means that the models accord with each other at large particle sizes, which is an indication of agreements in the inertial regime. This is because at a given frequency, the viscous boundary layer surrounding a particle is smaller for a larger particle than that for a smaller particle, and thus the particles perceive its surrounding liquid to be more inviscid.

To conclude, unlike in the case of attenuation, hydrodynamic interactions or multiple scatterings have little effect on the effective velocity, especially in the larger particle sizes.

4. Conclusions

In order to progress towards modeling viscous colloids, this paper has investigated ultrasonic attenuation and velocity of a suspension of solid spherical particles in a liquid using four different models. A hydrodynamic model, originally developed by Ament, been has been extended from low to high particle volume fraction by taking account of multi-particle interactions. Ultrasonic attenuation predictions from this model show excellent agreement with experimental data and with the results of the recently formulated multimodal multiple scattering model; in particular, for small particle sizes, this model is even found to predict attenuation better than that from the multiple scattering model. Findings from this paper also suggest that the core-shell model, inclusive of shear wave contributions, is not a good candidate to model attenuation for a dense suspension, although it can reliably predict ultrasonic velocity up to a certain volume fraction or frequency range. Our investigations also point out some flaws lying in the Harker and Temple model. This development of the hydrodynamic model at high particle concentration may find use in characterizing concentrated colloids. This model is a step forward towards applications in particle sizing instruments.

Acknowledgments

I acknowledge Prof Francine Luppé's earlier work with me that has helped develop ideas in this paper. I thank Prof Luc Mongeau (McGill University, Canada) and Dr. Oleg B. Gus'kov (Institute of Applied Mechanics, RAS, Russia) for supplying helpful comments on the dynamic drag.

References

[1] Dukhin, A. S.; Goetz, P. J. Applications for Dispersions. In *Characterization of Liquids, Dispersions, Emulsions, and Porous Materials Using Ultrasound*; Elsevier, 2017; pp 307–355. https://doi.org/10.1016/B978-0-444-63908-0.00008-9.

[2] Challis, R. E.; Povey, M. J. W.; Mather, M. L.; Holmes, A. K. Ultrasound Techniques for Characterizing Colloidal Dispersions. *Reports Prog. Phys.*, **2005**, *68* (7), 1541–1637. https://doi.org/10.1088/0034-4885/68/7/R01.

[3] Challis, R. E.; Pinfield, V. J. Ultrasonic Wave Propagation in Concentrated Slurries - The Modelling Problem We Dedicate This Paper to the Memory of Our Much Respected Friend and Colleague, the Late Dr. Bernard Hosten of the University of Bordeaux. *Ultrasonics*, **2014**, *54* (7), 1737–1744. https://doi.org/10.1016/j.ultras.2014.04.003.

[4] Epstein, P. S.; Carhart, R. R. The Absorption of Sound in Suspensions and Emulsions. I. Water Fog in Air. *J. Acoust. Soc. Am.*, **1953**, *25* (3), 553–565. https://doi.org/10.1121/1.1907107.

[5] Allegra, J. R.; Hawley, S. A. Attenuation of Sound in Suspensions and Emulsions: Theory and Experiments. *J. Acoust. Soc. Am.*, **1972**, *51* (5B), 1545. https://doi.org/10.1121/1.1912999.

[6] Hipp, A. K.; Storti, G.; Morbidelli, M. Acoustic Characterization of Concentrated Suspensions and Emulsions. 2. Experimental Validation. *Langmuir*, **2002**, *18* (2), 405–412. https://doi.org/10.1021/la015541w.

[7] Waterman, P. C.; Truell, R. Multiple Scattering of Waves. *Journal of Mathematical Physics*. 1961, pp 512–537. https://doi.org/10.1063/1.1703737.

[8] Fikioris, J. G.; Waterman, P. C. Multiple Scattering of Waves. II. "Hole Corrections" in the Scalar Case. *J. Math. Phys.*, **1964**, *5* (10), 1413–1420. https://doi.org/10.1063/1.1704077.

[9] Lloyd, P.; Berry, M. V. Wave Propagation through an Assembly of Spheres: IV. Relations between Different Multiple Scattering Theories. *Proc. Phys. Soc.*, **1967**, *91* (3), 678–688. https://doi.org/10.1088/0370-1328/91/3/321.

[10] Varadan, V. K.; Varadan, V. V.; Ma, Y. Multiple Scattering of Elastic Waves by Cylinders of Arbitrary Cross Section. II. Pair□correlated Cylinders. *J. Acoust. Soc. Am.*, **2005**, *78* (5), 1874–1878. https://doi.org/10.1121/1.392774.

[11] Linton, C. M.; Martin, P. A. Multiple Scattering by Multiple Spheres: A New Proof of the Lloyd--Berry Formula for the Effective Wavenumber. *SIAM J. Appl. Math.*, **2006**, *66* (5), 1649–1668. https://doi.org/10.1137/050636401.

[12] Norris, A. N.; Conoir, J.-M. Multiple Scattering by Cylinders Immersed in Fluid: High Order Approximations for the Effective Wavenumbers. *J. Acoust. Soc. Am.*, **2011**, *129* (1), 104–113. https://doi.org/10.1121/1.3504711.

[13] Lax, M. Multiple Scattering of Waves. II. the Effective Field in Dense Systems. *Phys. Rev.*, **1952**, *85* (4), 621–629. https://doi.org/10.1103/PhysRev.85.621.

[14] Caleap, M.; Drinkwater, B. W.; Wilcox, P. D. Coherent Acoustic Wave Propagation in Media with Pair-Correlated Spheres. *J. Acoust. Soc. Am.*, **2012**, *131* (3), 2036–2047. https://doi.org/10.1121/1.3675011.

[15] Ament, W. S. Sound Propagation in Gross Mixtures. *J. Acoust. Soc. Am.*, **2005**, *25* (4), 638–641. https://doi.org/10.1121/1.1907156.

[16] Austin, J. C.; Holmes, A. K.; Tebbutt, J. S.; Challis, R. E. Ultrasonic Wave Propagation in Colloid Suspensions and Emulsions: Recent Experimental Results. *Ultrasonics*, **1996**. https://doi.org/10.1016/0041-624X(95)00113-H.

[17] Valier-Brasier, T.; Conoir, J.-M.; Coulouvrat, F.; Thomas, J.-L. Sound Propagation in Dilute Suspensions of Spheres: Analytical Comparison between Coupled Phase Model and Multiple Scattering Theory. *J. Acoust. Soc. Am.*, **2015**, *138* (4), 2598–2612. https://doi.org/10.1121/1.4932171.

[18] Luppé, F.; Conoir, J.-M.; Norris, A. N. Effective Wave Numbers for Thermo-Viscoelastic Media Containing Random Configurations of Spherical Scatterers. *J. Acoust. Soc. Am.*, **2012**, *131* (2), 1113–1120. https://doi.org/10.1121/1.3672690.

[19] Luppé, F.; Valier-Brasier, T.; Conoir, J. M.; Pareige, P. Coherent Wave Propagation in Viscoelastic Media with Mode Conversions and Pair-Correlated Scatterers. *Wave Motion*, **2017**, *72*, 244–259. https://doi.org/10.1016/j.wavemoti.2017.03.002.

[20] Forrester, D. M.; Huang, J.; Pinfield, V. J.; Luppé, F. Experimental Verification of Nanofluid Shear-Wave Reconversion in Ultrasonic Fields. *Nanoscale*, **2016**, *8* (10), 5497–5506. https://doi.org/10.1039/c5nr07396k.

[21] Alam, M. M.; Pinfield, V. J.; Luppé, F.; Maréchal, P. Effective Dynamic Properties of Random Complex Media with Spherical Particles. *J. Acoust. Soc. Am.*, **2019**, *145* (6), 3727–3740. https://doi.org/10.1121/1.5111743.

[22] Coulouvrat, F.; Thomas, J.-L.; Astafyeva, K.; Taulier, N.; Conoir, J.-M.; Urbach, W. A Model for Ultrasound Absorption and Dispersion in Dilute Suspensions of Nanometric Contrast Agents. *J. Acoust. Soc. Am.*, **2012**. https://doi.org/10.1121/1.4765639.

[23] Harker, A. H.; Temple, J. A. G. Velocity and Attenuation of Ultrasound in Suspensions of Particles in Fluids. *J. Phys. D. Appl. Phys.*, **1988**, *21* (11), 1576–1588. https://doi.org/10.1088/0022-3727/21/11/006.

[24] Mei, R.; Lawrence, C. J.; Adrian, R. J. Unsteady Drag on a Sphere at Finite Reynolds Number with Small Fluctuations in the Free-Stream Velocity. *J. Fluid Mech.*, **1991**. https://doi.org/10.1017/S0022112091000629.

[25] Richardson, J. F.; Zaki, W. N. The Sedimentation of a Suspension of Uniform Spheres under Conditions of Viscous Flow. *Chem. Eng. Sci.*, **1954**. https://doi.org/10.1016/0009-2509(54)85015-9.

[26] Abbad, M.; Souhar, M. Experimental Investigation on the History Force Acting on Oscillating Fluid Spheres at Low Reynolds Number. *Phys. Fluids*, **2004**. https://doi.org/10.1063/1.1779051.

[27] Legendre, D.; Rachih, A.; Souilliez, C.; Charton, S.; Climent, E. Basset-Boussinesq History Force of a Fluid Sphere. *Phys. Rev. Fluids*, **2019**, *4* (7), 073603. https://doi.org/10.1103/PhysRevFluids.4.073603.

[28] Prasath, S. G.; Vasan, V.; Govindarajan, R. Accurate Solution Method for the Maxey-Riley Equation, and the Effects of Basset History. *J. Fluid Mech.*, **2019**. https://doi.org/10.1017/jfm.2019.194.

[29] Zuber, N. On the Dispersed Two-Phase Flow in the Laminar Flow Regime. *Chem. Eng. Sci.*, **1964**. https://doi.org/10.1016/0009-2509(64)85067-3.

[30] Sangani, A. S.; Zhang, D. Z.; Prosperetti, A. The Added Mass, Basset, and Viscous Drag Coefficients in Nondilute Bubbly Liquids Undergoing Small-Amplitude Oscillatory Motion. *Phys. Fluids A*, **1991**. https://doi.org/10.1063/1.857838.

[31] Biesheuvel, A.; Spoelstra, S. The Added Mass Coefficient of a Dispersion of Spherical Gas Bubbles in Liquid. *Int. J. Multiph. Flow*, **1989**. https://doi.org/10.1016/0301-9322(89)90020-7.

[32] Gus'Kov, O. B. The Virtual Mass of a Sphere in a Suspension of Spherical Particles. *J. Appl. Math. Mech.*, **2012**. https://doi.org/10.1016/j.jappmathmech.2012.03.007.

[33] Liu, C.; Li, Z. On the Validity of the Navier-Stokes Equations for Nanoscale Liquid Flows: The Role of Channel Size. *AIP Adv.*, **2011**. https://doi.org/10.1063/1.3621858.

[34] Hansen, J. S.; Dyre, J. C.; Daivis, P.; Todd, B. D.; Bruus, H. Continuum Nanofluidics. *Langmuir*, **2015**. https://doi.org/10.1021/acs.langmuir.5b02237.

[35] Forrester, D. M.; Pinfield, V. J. Shear-Mediated Contributions to the Effective Properties of Soft Acoustic Metamaterials Including Negative Index. *Sci. Rep.*, **2015**, *5* (November), 1–8. https:/doi.org/10.1038/srep18562.

[36] Kuster, G. T.; Toksöz, M. N. Velocity and Attenuation of Seismic Waves in Two□Phase Media: Part I. Theoretical Formulations. *Geophysics*, **1974**, *39* (5), 587–606. https://doi.org/10.1190/1.1440450.

[37] Batchelor, G. K. The Effect of Brownian Motion on the Bulk Stress in a Suspension of Spherical Particles. *J. Fluid Mech.*, **1977**. https://doi.org/10.1017/S0022112077001062.

[38] Dukhin, A. S.; Goetz, P. J. Acoustic Spectroscopy for Concentrated Polydisperse Colloids with High Density Contrast. *Langmuir*, **1996**. https://doi.org/10.1021/la951085y.

[39] Alam, M. M.; Pinfield, V. J.; Maréchal, P. Scattering Coefficients for a Sphere in a Visco-Acoustic Medium for Arbitrary Partial Wave Order. *Wave Motion*, **2020**, 102589. https://doi.org/10.1016/j.wavemoti.2020.102589.

[40] Forrester, D. M.; Pinfield V.; Luppé, F.; Huang, J.: Experimental verification of nanofluid shear-wave reconversion in ultrasonic fields: Dataset; Loughborough University, 2016. https://doi.org/10.17028/rd.lboro.2056149.v1

[41] Alam, M. M.; Data for: Ultrasonic propagation in concentrated colloidal dispersions: improvements in a hydrodynamic model. Mendeley Data, 2020. https://data.mendeley.com/datasets/zjfh6m67kc/1

Appendix

The monopole and dipole scattering coefficients for a sphere

The scattering coefficients of a sphere are obtained by imposing the displacement and stress continuity conditions at the interface between the particle and the surrounding material and then solving the resulting boundary equations; the details can be found in the Refs. [5, 39].

For the monopole mode ($n = 0$), the compressional wave exists only, but for the dipole mode ($n = 1$), or higher-order modes, both compressional and shear waves exist. The monopolar scattering coefficient is

$$T_0^{cc} = \frac{\frac{\hat{\rho}}{(k_s'a)^2}[\,(k_s'a)^2 j_0(k_c'a) + 4k_c'a\, j_0'(k_c'a)]k_c a\, j_0'(k_c a) - \frac{1}{(k_s a)^2}[\,(k_s a)^2 j_0(k_c a) + 4k_c a\, j_0'(k_c a)]k_c'a\, j_0'(k_c'a)}{\frac{1}{(k_s a)^2}[\,(k_s a)^2 h_0(k_c a) + 4k_c a\, h_0'(k_c a)]k_c'a\, j_0'(k_c'a) - \frac{\hat{\rho}}{(k_s'a)^2}[\,(k_s'a)^2 j_0(k_c'a) + 4k_c'a\, j_0'(k_c'a)]k_c a\, h_0'(k_c a)} \tag{A1}$$

The dipolar scattering coefficients for both compressional and shear waves are

$$T_1^{cc} = -\frac{i(k_c a)^3[\,h_1(k_s a) - k_s a\, h_1'(k_s a)](\hat{\rho} - 1)}{3\delta}, \tag{A2}$$

$$T_1^{cs} = -\frac{i\, k_c a(\hat{\rho} - 1)}{\delta}, \tag{A3}$$

$$T_1^{sc} = \frac{2(\hat{\rho} - 1)(k_c a)^2}{\delta}, \tag{A4}$$

$$T_1^{ss} = -\frac{[\,(4\hat{\rho} - 7)j_1(k_s a) + (2\hat{\rho} + 1)\, k_s a\, j_1'(k_s a)]}{\delta}, \tag{A5}$$

$$\text{with} \quad \delta := (4\hat{\rho} - 7)h_1(k_s a) + (2\hat{\rho} + 1)\, k_s a\, h_1'(k_s a). \tag{A6}$$

The scattering coefficients are obtained assuming long-compressional wavelength limit, while imposing no restriction on the shear wavelength in the liquid. In the long-wavelength approximation, only the monopole and dipole scattering coefficients are dominant. [2, 4, 5]

When the scattering coefficients are used for the core-shell system, one needs to replace the particle radius a with the shell radius $b\,(= a\varphi^{-1/3})$.